



**HAL**  
open science

## Accurate Transient Behavior Measurement of High-Voltage ESD Protections Based on a Very Fast Transmission-Line Pulse System

Antoine Delmas, Nicolas Nolhier, David Trémouilles, Marise Baffleur, Nicolas Mauran, Amaury Gendron

► **To cite this version:**

Antoine Delmas, Nicolas Nolhier, David Trémouilles, Marise Baffleur, Nicolas Mauran, et al.. Accurate Transient Behavior Measurement of High-Voltage ESD Protections Based on a Very Fast Transmission-Line Pulse System. 31st Electrical Overstress/Electrostatic Discharge Symposium, 2009. EOS/ESD Symposium, Aug 2009, ANAHEIM, United States. pp.165-172. hal-00445676

**HAL Id: hal-00445676**

**<https://hal.science/hal-00445676>**

Submitted on 11 Jan 2010

**HAL** is a multi-disciplinary open access archive for the deposit and dissemination of scientific research documents, whether they are published or not. The documents may come from teaching and research institutions in France or abroad, or from public or private research centers.

L'archive ouverte pluridisciplinaire **HAL**, est destinée au dépôt et à la diffusion de documents scientifiques de niveau recherche, publiés ou non, émanant des établissements d'enseignement et de recherche français ou étrangers, des laboratoires publics ou privés.

# Accurate Transient Behavior Measurement of High-Voltage ESD Protections Based on a Very Fast Transmission-Line Pulse System

Antoine Delmas (1)(2)(3), David Trémouilles (1)(2), Nicolas Nolhier (1)(2), Marise Bafleur (1)(2), Nicolas Mauran (1)(2) Amaury Gendron (4)

(1) CNRS; LAAS; 7 avenue du Colonel Roche, F-31077 Toulouse, France

(2) Université de Toulouse; UPS, INSA, INP, ISAE, LAAS, F31077 Toulouse, France

(3) Freescale Semiconductor Inc.; TSO; 134 avenue du Général Eisenhower, 31023 Toulouse, France

(4) Freescale Semiconductor Inc.; TSO; 2100 East Elliot Road, Tempe, AZ-85284, USA

**Abstract** – A comprehensive study of the limitations of vf-TLP setup for transient measurements is exposed. A new method, based on a numerical correction of measured data using a commercial Oryx vf-TLP system is presented. It allows the measurement of ESD pulses up to 1000 V with a time resolution down to 60 ps.

## I. Introduction

Design of efficient integrated ESD protections in high voltage technology (HV) is still a real challenge to fulfill the constraints of severe environments such as automotive. Up to now no measurement tool is available to accurately assess the transient behavior of high voltage ESD protection devices. Very fast transient behavior measurement setups have been reported during the last few years [1,2]. However, their maximum voltage limitation ( $\sim 50$  V for most advanced solid-state pulse generators) does not allow characterizing high voltage protection devices.

We have analyzed the limitations of a commercial Oryx TLP system for transient measurement analysis and have developed a new accurate method to extract transient device behavior from this standard vf-TLP test bench. Both aspects are brought up in this paper.

In section two, the vf-TLP system used is described. Its operation and the limitations for transient analysis are analyzed in section three. Finally, the new method to obtain accurate transient information is presented and validated on HV bipolar protection devices.

## II. The very fast-TLP system in TDR configuration

The commercial Oryx Celestron vf-TLP system is capable of generating short pulses down to 1.25 ns

duration, with rise-times shorter than 100 ps. As described in figure 1, it is composed of a coaxial line (TL1) charged by a high voltage source through a high value resistor. With the TL1 used, a 5 ns pulse is produced at each closing of the switch. It then propagates through TL2, and reaches a voltage and a current probe.

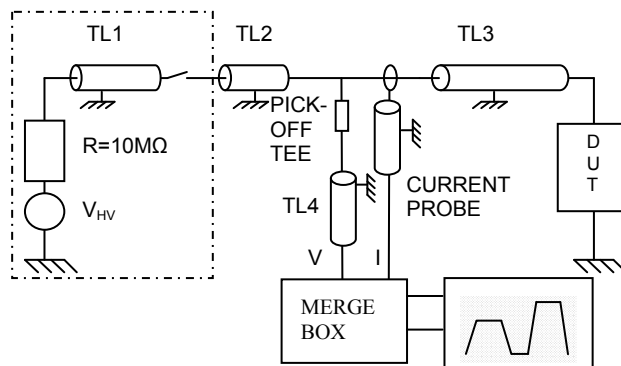


Figure 1 : TDR vf-TLP set-up.

The measured signal is sampled by a TDS6604C Tektronix real-time oscilloscope with an analog bandwidth of 6 GHz. The pulse then flows through TL3 to the device under test, where it is partially reflected depending upon the DUT impedance. The reflected pulse is also measured by the oscilloscope.

This system then gives an image of both the incident and the reflected pulse at the DUT, separated by a time delay. The DUT voltage and current can be

calculated as a sum of these two components after time alignment:

$$\begin{cases} V_{DUT} = V_{inc} + V_{ref} \\ I_{DUT} = I_{inc} + I_{ref} \end{cases} \quad (1)$$

The superposition of the incident and reflected pulses, occurring at the DUT, can be recreated using the “merge box” included in the commercial Oryx vf-TLP bench [3]. Its effect is to delay the incident pulse so that the incident and reflected pulses reach the oscilloscope at the same time.

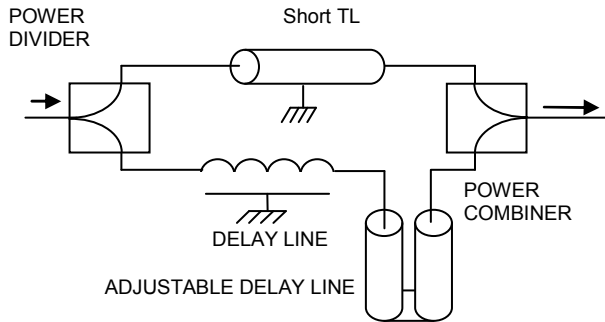


Figure 2: Operation of the "merge box"

This “merge box” is inserted in series in between the voltage and current probes and the oscilloscope. As represented in figure 2, a 6 dB power divider splits the signal into two components. One of these components is directly transmitted to the oscilloscope, while the other is conducted to a fixed 15 ns delay line and a line stretcher with a 630 ps range, allowing a precise adjustment of the delay applied on the incident pulse.

The delay is generally tuned visually by measuring the voltage on a short-circuit and the current on an open circuit. The superposition of the delayed incident pulse and the reflected pulse is adjusted to be equal to zero.

### III. Operation and limits

The vf-TLP system described in the previous section is perfect for quasi-static measurements. The quasi-static voltage and current values are evaluated from an averaging of the measurements recorded during the last nanoseconds of the waveform. The averaging window can be tuned by the user, in order to avoid misalignment problems. A full “multi-point” calibration of the bench can also be done before the measurements, to partially correct the errors brought by the attenuation through the cables.

However, there are two sources of errors, mismatch issues between incident and reflected pulses and the filtering of the signal by the measurement setup, which become major concerns when making transient measurements.

### A. Evaluation of the alteration caused by the set-up on the signal

The system itself filters the signal, which is the main reason for the signal alteration. The cables, voltage and current probes as well as the merge box induce various signal attenuations.

#### 1. Frequency dependant attenuation from the coaxial cables and the merge box

The error from the non-ideality of the coaxial cables has to be taken into account since significant lengths of cable are used. Indeed, the incident pulse measured on the scope undergoes attenuation from TL2, TL4 (fig.1) and the internal delay line and line stretcher from the merge box (fig. 2), while the reflected pulse is attenuated by TL2, TL3 twice, and TL4. In comparison, the pulse, when arriving on the device under test, is only attenuated by TL2 and TL3. TL2, TL3 and TL4 are of the same cable type, (0.25 dB/m attenuation at 1 GHz), while the delay line and the line stretcher from the merge box have a weaker attenuation coefficient (0.22 dB/m at 1 GHz).

Altogether, for example at 1GHz, the attenuation brought by the cables from the generator to the scope is approximately 0.85 dB for the incident pulse, 0.90 dB for the reflected pulse, while the attenuation on the signal when it reaches the device is only 0.45 dB, which means that the error is approximately 0.40 dB and 0.45 dB respectively for the incident and reflected pulses at this frequency. Moreover, the frequency dependant attenuation and frequency dispersion of the signal bring a quite important error in the measurement of the DUT’s transient behavior.

#### 2. Filtering from the voltage and current probes

The non-ideal frequency response of the probes is another source of error. Indeed, the voltage and current probes are respectively a pick-off tee and a current transformer, whose frequency transmission characteristics are represented on fig. 3. The cutoff frequency (2-3GHz) of the current probe is too low and its attenuation too important at high frequencies to use it as a precise transient characterization vf-TLP

tool. But the voltage probe is suitable for pulses with frequency components less than 3 GHz. The voltage probe (resistive pick-off tee) presents capacitive coupling effects between its input and its output, which explains its increasing transmission coefficient with increasing frequencies.

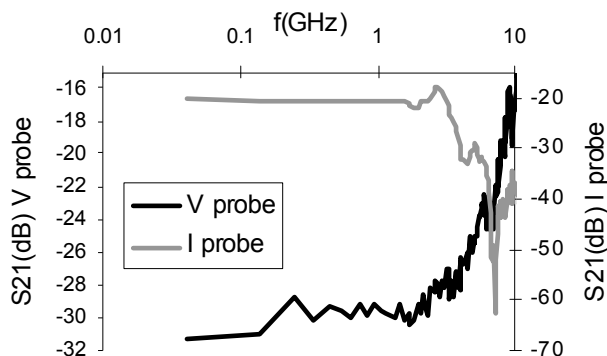


Figure 3: Frequency transmission coefficients of the voltage and current probes. The current probe has a 2 GHz cutoff frequency. The voltage probe has a 3 GHz cutoff frequency.

### 3. Results of the distortion by the cables, the voltage probe and the merge box

The merge box has a strong impact on the signal. The power dividers, the line stretcher and the delay line bring important attenuation and distortion. When added to the filtering from the probes and from the coaxial cables, this distortion can change a square pulse into a “RC load” type waveform, as can be seen on fig. 4.

Figure 4 shows a comparison between a 5V pulse measured directly at the end of TL3 (figure 1), before reaching the DUT ( $V_{inc,DUT}$ ), and another 5V pulse, distorted by both the vf-TLP measurement box and the merge box ( $V_{inc,meas}$ ). The latter one has been multiplied by a factor 120, as done in the Oryx software, to correct the data from the  $\pm 30$  division of the pick-off tee, and the two  $\pm 2$  divisions of the merge box’s power splitters.

A good calibration of the setup can be done, based on a point-by-point characterization, using both an open-circuit and a short-circuit. In the case above, the measured waveform has to be corrected by a calibration parameter in order to reach a 5V value on the plateau. This correction is suitable for quasi-static measurements if the calibration and the measurement are done using the same sampling window, but is not sufficient for transient measurements, since, as we can see, the difference between the measured signal and the real one is time-dependant, and seems to stabilize only after approximately 5 ns.

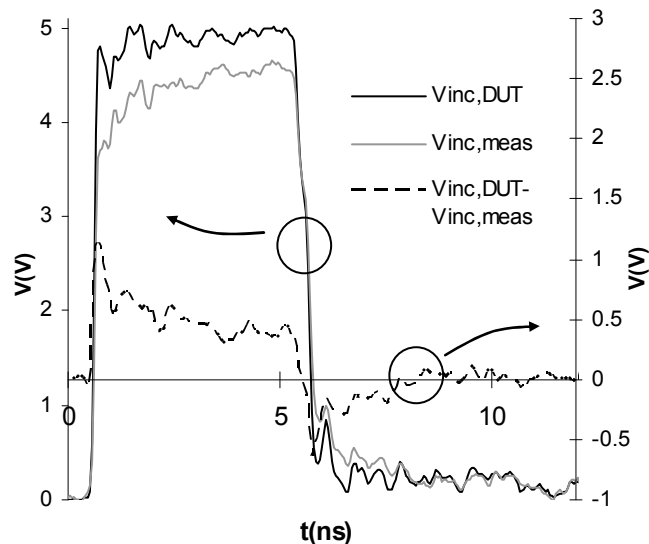


Figure 4: incident waveforms measured as seen by the DUT ( $V_{inc,DUT}$ ), and at the output of the merge box, as seen by the oscilloscope ( $V_{inc,meas}$ ). The distortion on the measured signal is visible.

### B. Delay adjustment issues

As developed previously, the adjustment of the merge box voltage channel delay can be done by measuring the voltage on a short-circuit. A micrometric screw allows this adjustment with a resolution of 5 ps. One can consider that the fit is done when the positive and negative peaks caused by the mismatch of the incident and reflected pulses are cancelled.

However, a certain range remains, where these peaks are surrounded by noise, which makes them harder to detect. Moreover, most of the time, a slowly decreasing residual voltage, due to the non-zero spark resistance in the switch pulse generator, can be present long after the fall of the incident pulse, and can reach up to 10% of the pulse’s amplitude. This residual voltage is superimposed on the measurement noise, and, altogether, this brings an important source of error for the delay adjustment.

As an example, let us consider a 100V pulse with a 1 ns rise-time, a 1 V amplitude noise, and a 9 V residual voltage  $V_R$  (Fig. 5). The uncertainty on the delay fit can be approximated by:

$$\Delta t = \frac{V_R + noise}{dV/dt} = 100 ps \quad (2)$$

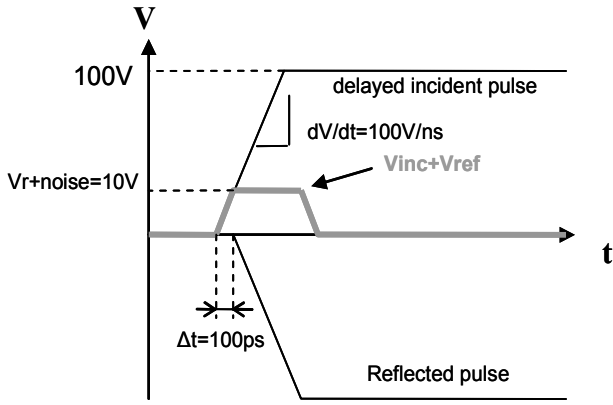


Figure 5: Schematic representation of the uncertainty in the adjustment of the merge box delay, in a particular case.

## IV. A new methodology for measured data correction

The solution we developed to solve the problems cited above is based on a mathematical post-processing of the data measured with the oscilloscope. The accuracy of the measurements is greatly enhanced, so that the actual limitation for precise measurements is the 6 GHz analog bandwidth of the oscilloscope, which corresponds to a 58 ps rise-time.

### C. Principles of the method

The proposed method is somewhat similar to the one applied on a TLP bench in [1]. However, the separation of incident and reflected pulses in vf-TLP leads to a different treatment in the measurement data. Moreover, the use of wafer RF probes simplifies the problem, since no parasitic inductance has to be taken into account.

The setup has been reduced to the voltage pick-off tee, avoiding the problems of the merge box and the current probe. The current probe is not necessary, since the current can be calculated from the voltage measurements, as shown below (equation 8).

The principle is as follows: the set-up can be considered as a 3-port system, with the corresponding transmission coefficients  $S_{21}$ ,  $S_{31}$ , and  $S_{32}$  (fig.6).

The frequency losses due to the different parts of the system and the propagation delays are fully characterized in the frequency domain by the S-parameter coefficients of the different wave paths (fig. 6).

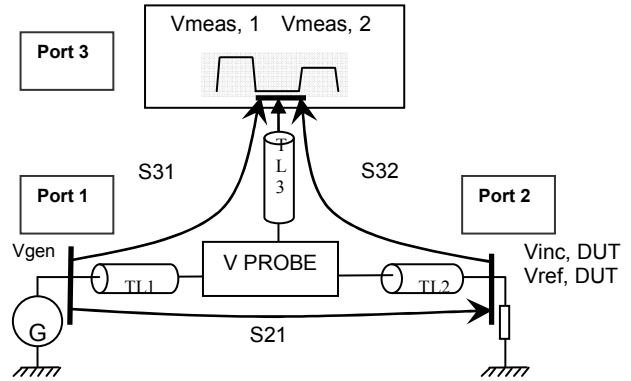


Figure 6: Schematic representation of the S parameters measured.

We can use these coefficients to recalculate the real voltage and current waveforms as seen by the DUT. Indeed, in the frequency domain, since all the transmission lines have a  $50 \Omega$  characteristic impedance ( $Z_c$ ) in the frequency range used for the calculation, the injected voltage  $V_{gen}$ , the incident ( $V_{inc,DUT}$ ) and reflected ( $V_{ref,DUT}$ ) pulses at the DUT can be directly computed from the measured incident ( $V_{meas,1}$ ) and reflected ( $V_{meas,2}$ ) pulses, using the transmission coefficient  $S_{32}$ ,  $S_{21}$  and  $S_{31}$  (measured with a Vector Network Analyzer) in the following way:

$$\begin{cases} V_{inc,DUT}(f) = S_{21} V_{gen}(f) \\ V_{gen}(f) = \frac{1}{S_{31}} V_{meas,1}(f) \end{cases} \quad (3)$$

with  $V_{meas,1}$  and  $V_{meas,2}$  the incident and reflected pulses measured on the scope (fig. 6).

$$\Rightarrow V_{inc,DUT}(f) = \frac{S_{21}}{S_{31}} V_{meas,1}(f) \quad (4)$$

Then, with

$$V_{ref,DUT}(f) = \frac{1}{S_{32}} V_{meas,2}(f) \quad (5)$$

we obtain:

$$V_{DUT}(f) = V_{inc,DUT}(f) + V_{ref,DUT}(f)$$

$$\boxed{V_{DUT}(f) = \frac{S_{21}}{S_{31}} V_{meas,1}(f) + \frac{1}{S_{32}} V_{meas,2}(f)} \quad (6)$$

Then, with

$$\begin{cases} I_{inc,DUT}(f) = \frac{V_{inc,DUT}(f)}{Z_c} \\ I_{ref,DUT}(f) = -\frac{V_{ref,DUT}(f)}{Z_c} \end{cases} \quad (7)$$

$$I_{DUT}(f) = \frac{1}{Z_C} (V_{inc,DUT}(f) - V_{ref,DUT}(f)) \quad (8)$$

Transformations from the time domain to the frequency domain and from the frequency domain to the time domain are being done respectively by means of fast Fourier transformation and inverse fast Fourier transformation algorithms.

The measured signal has first to be split into its two “incident” and “reflected” components. These two pulses have to be well separated for an accurate extraction of the reflected pulse. To do so, one can extend the “TL2” coaxial cable between the pick-off tee and the DUT (fig.6). But the overlap of the incident pulse on the reflected one can also be corrected using additional calculations.

S-parameter measurements were performed using a 9kHz-4GHz ZVRE Rohde & Schwartz VNA for low frequencies and a 40 MHz-40 GHz 37369c Anritsu VNA for higher frequencies. Since the wafer RF probes cannot be easily characterized in the frequency domain, they were not included in the measurements, but approximated by an ideal 80 ps delay, measured in the time domain (vf-TLP).

The principle of the method is based on the hypothesis according to which the S-parameter coefficients of the system do not depend on the injected power, so that it will react similarly to a 0.1 mW sinusoidal signal (from a VNA) and to a 500 V vf-TLP pulse.

This hypothesis of the “power linearity” of the voltage probes cannot be verified with a VNA, since none of these tools is capable of injecting power as great as those encountered during vf-TLP measurements.

But it is possible to inject vf-TLP pulses from the input (port 1 from fig. 6), and to compare the spectra of the pulses obtained at the 2 different outputs of the system (port 2 and 3 from fig. 6). This was made for four voltages between 10V and 180V. Fig. 7 shows a comparison of the ratio  $V_{Port2}/V_{Port3}$  for these different voltages. The pulses obtained at these two ports were measured simultaneously on two different channels of the scope, and their spectra were obtained from fast Fourier transformations.

This  $V_{Port2}/V_{Port3}$  ratio seems to stay constant whatever the injected power, which indicates that the voltage probe’s behavior is linear for increasing powers.

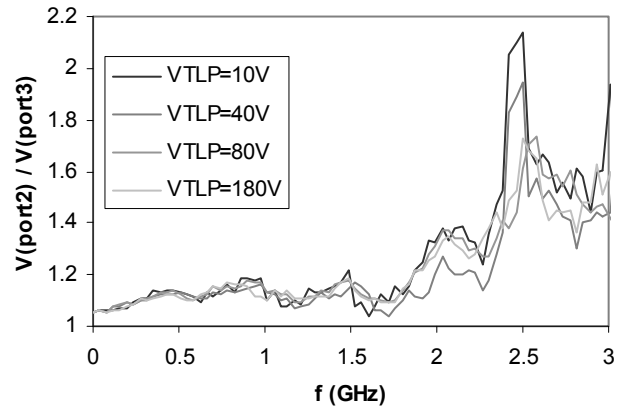


Figure 7: Measurement of the linearity of the voltage probe for different input voltages, from 10V to 180V. A 30 dB attenuator with a 12 GHz pass band was inserted after port 2 to protect the input of the oscilloscope.

## D. Application on ESD protections testing

The easiest way to test the accuracy of the new method is to make a measurement on an open circuit and to calculate the incident and reflected pulse waveforms as seen by the open circuit (fig. 8 and 9)

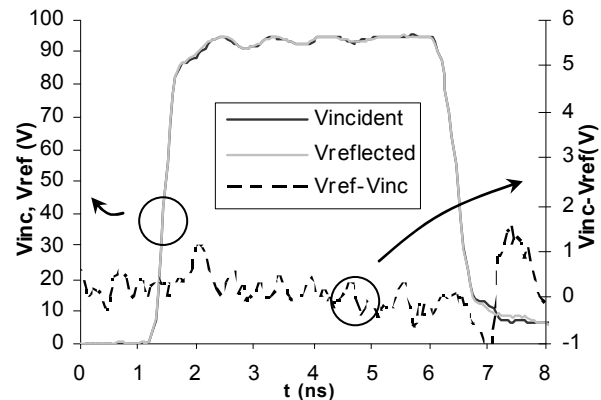


Figure 8: Comparison of the waveforms calculated for the incident and reflected pulses on an open circuit.

These two waveforms being obtained from two different paths according to equations 4 and 5, ( $S_{21}$  and  $S_{31}$  for the incident wave and  $S_{32}$  for the reflected one), their good superposition ( $\sim 1\%$  error) allows us to trust the accuracy of the method.

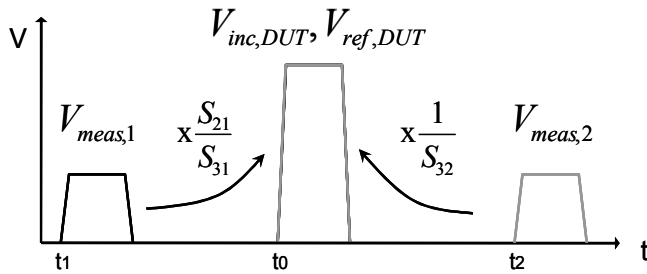


Figure 9: Calculation of the incident and reflected pulses on a perfect open-circuit. In this case, the two pulses should be equal and perfectly aligned in time.

The accuracy of the method for quasi-static measurement has been tested too, both on a short-circuit and on an open-circuit, between 1 V and 1000 V TLP (fig. 10). The results showed a less than 300 mΩ resistance for the short-circuit, and a more than 7 kΩ resistance for the open-circuit. Here, the main limitation is the 8 bits coding of the vertical range of the scope, which leads to a 4 V vertical resolution in the case of a 1000 V TLP pulse.

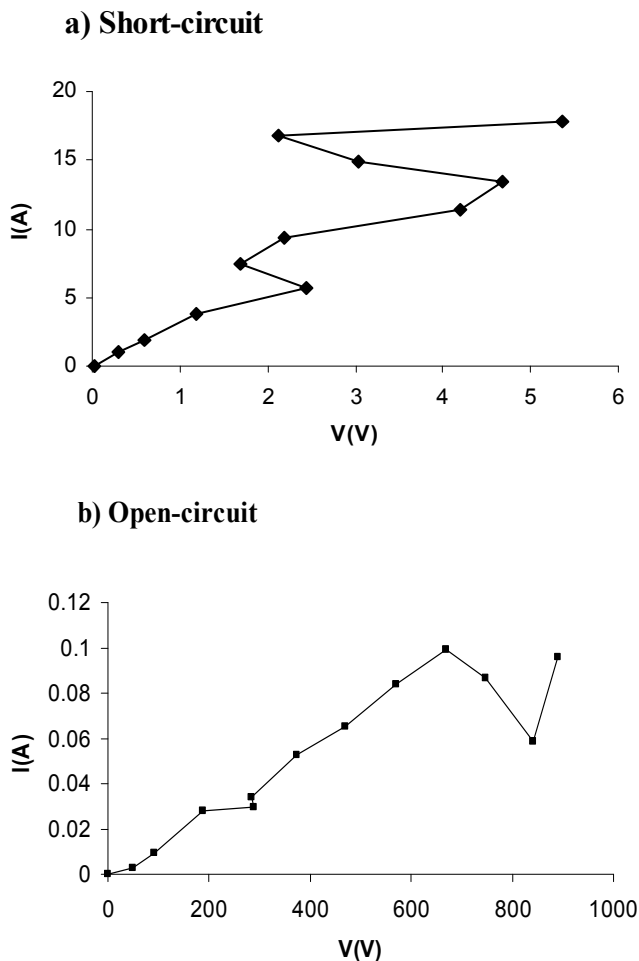


Figure 10: vf-TLP-type measurement results obtained by averaging  $V(t)$  and  $I(t)$  plots at different TLP voltages, on a short-circuit (a), and on an open-circuit (b).

Figure 11 shows a series of vf-TLP measurements at 250 V precharge voltage on a 40 V grounded NPN bipolar protection in a Smart Power technology, with different rise times. The observed increasing of the overshoot with decreasing rise times corresponds to the 2D TCAD simulation predictions.

Fig. 12 shows a comparison between corrected data and data measured using the classical set-up, including the merge box. We can observe the effects of signal filtering on the aspect of the “ $V_{\text{measured } 1}$ ”, “ $V_{\text{measured } 2}$ ” and “ $V_{\text{corrected}}$ ” curves: the 240 V/ns  $dV/dt$  slope of the measured data is increased by a factor 25% in the corrected data, and the holding voltage is decreased by 15%. The error in the holding voltage of the measured data can then be corrected for quasi-static measurements, as explained in section III.A.

A bad adjustment of the merge box’ delay can also lead to important errors in the extraction of the overshoot peak maximum voltage (15 % error in our case).

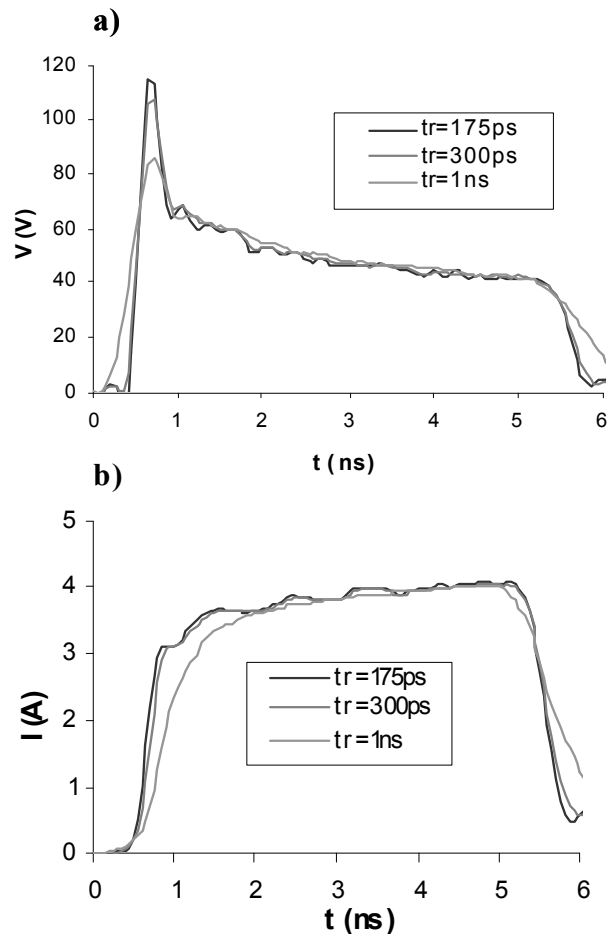


Figure 11: voltage (a) and current (b) waveforms obtained on a NPN bipolar protection at 250 V, with rise-times between 175 ps and 1 ns.

Figure 13 shows a series of measurements on two grounded NPN bipolar protections, DUT1 and DUT 2, in a Smart Power technology. The two components are identical except for their base doping, DUT 2 having a more heavily doped base than DUT1. This leads to a different behavior, such as a different breakdown voltage (17 V for DUT1 and 22 V for DUT2) and a different on-state resistance (9  $\Omega$  for DUT1 and 7  $\Omega$  for DUT2).

Transient vf-TLP measurements were done for different current levels, and the peak maximum voltage  $V_{max}$  was extracted for every current level. The results are plotted on fig. 13, with the maximum voltage  $V_{max}$  on the x-axis, and the quasi-static current  $I$  on the y-axis. The quasi-static I-V curves were plotted for comparison.

As we can see, DUT 1 presents a lower overshoot at every current level than DUT 2, despite its bigger on-state resistance. This could be explained by its lower base doping, which leads to a greater diffusion coefficient of the electrons through the base  $D_{nBase}$ , and thus to a smaller transit time of the electrons through the base  $\tau_{eB}$ , as can be seen in equation 9.

$$\tau_{eB} = \frac{W_B^2}{4D_{nBase}} \quad (9)$$

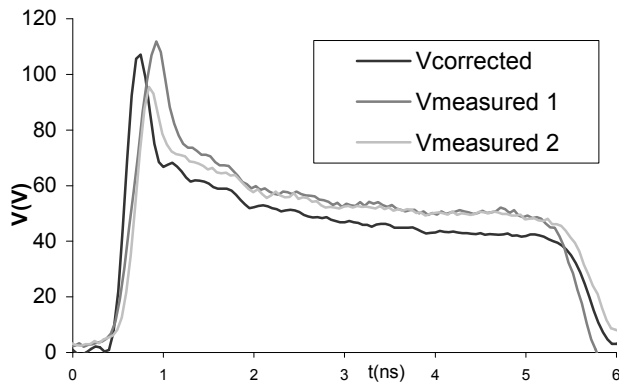


Figure 12: Voltage measurements obtained on the same device, with a 300 ps rise-time. The black curve represents the voltage obtained with the described method. The two other curves represent data measured using the conventional set-up, with a 150 ps delay difference in the merge box adjustment.

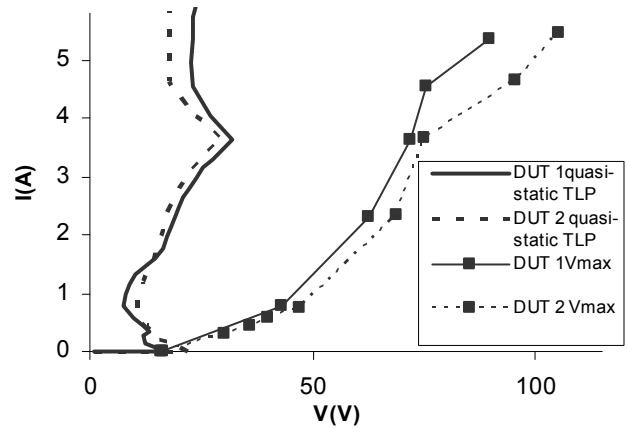


Figure 13: Quasi-static and transient measurements on two NPN devices with different base dopings.

## V. Conclusion

In this paper, a simple post-processing method for the measurement of high voltage transients was presented. The limits of actual commercial vf-TLP systems were first exposed, and the basis of the method was explained. The validation on simple cases and on an ESD protection device was shown.

One of the main advantages of this method is the possibility of its realization with a standard commercial vf-TLP bench. The actual limitations for the precision of the results are the 6 GHz analog bandwidth of the oscilloscope and its 8 bits coding of the measured voltage, which only brings a 4 V resolution in the case of a 500 V incident pulse amplitude (1000 V TLP).

## Acknowledgements

The authors would like to gratefully acknowledge Evan Grund for bringing his knowledge and experience on the vf-TLP system while mentoring this paper.

## References

- [1] H. Wolf, H. Gieser, "Transient Analysis of ESD Protection Elements by Time Domain Transmission Using Repetitive Pulses", EOS/ESD 2006, pp. 304.
- [2] Manouvrier, J.-R.; Fonteneau, P.; Legrand, C.-A.; Nouet, P.; Azais, F., "Characterization of the transient behavior of gated/STI diodes and their



associated BJT in the CDM time domain,"  
EOS/ESD 2007, pp.3A.2-1-3A.2-10, 16-21 Sept.  
2007.

- [3] E. Grund, "Deriving the DUT Current and Voltage Waveforms by Merging VF-TLP Incident and Reflected Signals", Proceedings of the 3rd EOS/ESD/EMI Workshop, Toulouse France, May 2006.
- [4] D. Tremouilles, S. Thijs, Ph. Roussel, M.I. Natarajan, V. Vassilev, G. Groeseneken, *Transient voltage overshoot in TLP testing - Real or artifact?*, Microelectronics Reliability, Volume 47, Issue 7, Special Issue: EOS/ESD Symposium 2005, July 2007, Pages 1016-1024